Influence of water ageing on the mechanical properties of flax/PLA non-woven composites

Delphin Pantaloni, Alessia Melelli, Darshil U. Shah, Christophe Baley, Alain Bourmaud

Influence of water ageing on the mechanical properties of flax/PLA non-woven composites

Delphin Pantaloni[a], Alessia Melelli[a], Darshil. U. Shah[b], Christophe Baley[a] and Alain Bourmaud[a]

a : Université de Bretagne-Sud, IRDL, CNRS UMR 6027, BP 92116, 56321 Lorient Cedex, France

b : Centre for Natural Material Innovation, Department of Architecture, University of Cambridge, Cambridge CB2 1PX, United Kingdom

* Corresponding author: alain.bourmaud@univ-ubs.fr Tel.: +33-2-97-87-45-18

Abstract

Flax fibres are widely used in the automotive sector to reinforce polyolefins, such as for dashboard and interior door panels. A promising option is poly-(lactid) (PLA), as it leads to higher mechanical properties and offers an additional end-of-life scenario following recycling: industrial composting. However, like other composite systems such as flax/polyolefin, flax/PLA composites are also sensitive to water. Here, a non-woven flax/PLA composite is aged under several conditions (50% RH/75% RH/98% RH/Immersion) until saturation. After ageing, all samples are reconditioned at 50% RH, and their residual properties are assessed. The presence of a critical relative humidity between 75% and 98% is highlighted, above which, increases in moisture content irreversibly decrease the composite's mechanical properties. After ageing at 98% RH and in immersion, tangent modulus was reduced by 23.0 and 33.8% and ultimate strength by 26.7 and 37.4%, respectively, compared to reference materials. This decrease is mainly due to microstructure evolution in the form of increasing porosity. This microstructure evolution is induced by the swelling of flax fibres, which generates high local stresses, above what PLA can withstand. As a result, micro-cracks appear in the matrix, responsible for reduction in mechanical properties.

Keywords : Biocomposites ; Flax fibres ; Non-woven ; Degradation ; Microstructure ; Moisture

1 Introduction

Thanks to their light weight [1] and their good mechanical properties [2], flax fibres can be drop-in alternatives to glass fibres as composite material reinforcements in the automotive area [3]. In addition, using thermoplastics as matrices reduces the composite's environmental impacts, especially thanks to recycling [4], which is a potential end-of-life solution for circularity. However, one of the bottlenecks for wider applications is the sorption behaviour of flax composites, especially when considering stringent validation standards of the automotive industry, which impose the test of materials across a large range of humidity and temperature conditions [5].

An elementary flax fibre, not embedded in a matrix, has a moisture content of 6% at 50% relative humidity (RH) and reaches 18% at 98% RH [6]. Flax sorption behaviour follows Park's model [7,8], divided into three sorption mechanisms, depending on the relative humidity. The first part follows Langmuir's sorption, where water molecules attach on specific sites of interactions. The second is described by Henry's sorption, where water uptake evolves linearly with the relative humidity, and the final stage occurring at high relative humidity is the clustering of water molecules in the remaining free spaces. Combining these three phenomena leads to a sigmoidal relation between the relative humidity and the moisture content in the flax fibres [6]. Interestingly, this phenomenon presents a hysteresis loop meaning that the water content of flax is not the same at a given relative humidity depending on if it is in the dynamic state of sorption or desorption [6]. Furthermore, this water uptake induces radial swelling of the flax fibre, correlating linearly with the hygro-expansion coefficient, measured to be 1.14 $\varepsilon/\Delta m$ by Le Duigou et al. [9].

The moisture uptake in a composite is mainly due to flax fibres' water sorption behaviour and

47 the presence of a fibre/matrix interface [10], even for a hydrophilic matrix (PHBV) [11]. The
48 sigmoidal sorption/desorption behaviour is also observed at the composite level [5]. For non-
49 woven flax/PP composite (50wt%), Gager et al. [5] report a moisture content of 2.6% at 50%
50 RH and 8% at 98% RH. The volume fraction of fibres impacts the moisture sorption of the
51 composites [12]. However, the classical rule of mixture cannot predict the moisture uptake of
52 the composites at high relative humidity. It appears coherent with experimental values at 75%
53 RH but overestimates them at 98% RH [12]. This deviation at high relative humidity is
54 explained by El Hachem et al. [12] by the containment effect of the matrix on the flax fibres,
55 limiting their moisture uptake potential. Indeed, flax swelling is observed at the composite
56 scale at a lower amplitude, as the matrix constrains fibre displacement [13].

57 This moisture uptake induces a decrease in stiffness and ultimate strength of the composite
58 [5,10,14]. The origin of this decrease is still discussed in the literature [15–17], and several
59 phenomena appear to be involved. It is reported for thermoset flax composites that cracks
60 appear in the matrix [14,17], inducing debonding at the flax/matrix interface [14,15,17] and
61 flax fibre damage [15,17,18]. All these phenomena are reported to be linked with the swelling
62 of flax fibres inside the composite. However, there is no consensus because the phenomena
63 observed varies depending on the ageing conditions, the experimental methods, and the flax
64 composite mesostructure such as porosity, fibre volume fraction, fibre individualisation and
65 fibre orientation. As an example, Chilali et al. [19] observed that the presence of sealed edges,
66 inducing a preferential water diffusion direction, impacts the sorption kinetics and the ageing
67 behaviour. Indeed, they suggest several damage mechanisms depending on the type of
68 diffusion.

69 This paper focuses on the hygroscopic ageing of flax/PLA non-woven composite through its
70 mesostructure and mechanical property evolution. Several hygroscopic conditions are

investigated (50% RH / 75% RH / 98% RH) as well as immersion ageing. The sorption kinetics are followed through weight monitoring, and the residual composite mechanical properties are measured. The mechanical properties of flax cell walls and matrix after ageing are also investigated at microscale thanks to AFM Peakforce measurements in mechanical mode (AFM-PF-QNM). Finally, the structure of the composite is examined through density measurement and SEM observation.

2 Materials and methods

2.1 Materials

2.1.1 Raw materials

An industrial non-woven flax/PLA preform of 350 g/m² with a flax weight fraction of 40%, was manufactured on a needle-punching industrial line (Ecotechnilin, Yvetot, France). The non-woven has a preferred fibre direction. Indeed, the machine direction has slightly more oriented fibres in these industrial non-wovens [20]. The raw materials used are scutched flax tows and INGEO™ PLA fibres. Thanks to the needle-punching line, flax and PLA fibres are commingled together, leading to the non-woven preform.

2.1.2 Composite manufacturing

Composite manufacturing is done through an optimised thermo-compression cycle of eight minutes using a hydraulic press LabTech Scientific 50T (Labtech, Samutprakarn, Thailand) press, set at 200°C. This processing cycle is presented in a previous study [21]. Eight plies of 200x200 mm are stacked together and then dried at 40°C under vacuum for 24h. During the lay-up step, the specific orientation of the preforms is maintained. Therefore, thermo-compression leads to a composite with a preferential orientation of fibres, identical to the preform.

Next, dog-bone samples, according to the ISO 527-4 standard, are cut from the 2 mm thick

composite plates using a milling machine. The centre part of the dog bone has a width of 8 mm, a length of 45 mm and a thickness of 2 mm. The edges of the samples were not sealed to be consistent with industrial applications. Thus, after cutting, flax fibres appear accessible in the edges. Furthermore, the milling process damages the edges by initiating defects, which are likely to influence the ageing response of the composite.

2.2 Methods

2.2.1 Ageing protocol

Once manufactured, samples are stored in a controlled humidity chamber at 50% RH. Once the weight is stabilised, five samples are dried for 48h in an oven at 105°C and weighted. The initial moisture content of samples, obtained through the mean of the five values, is 2.6 ± 0.1 %. The remaining samples are separated into fives batches. One stays in the 50% RH chamber until the end of the experiments and is called the 50_RH_ref batch. Others undergo humidity ageing (also called vapour ageing) at 50%, 75% or 98% RH thanks to humidity chambers (corresponding batches are labelled 50_RH/ 75_RH/ 98_RH) or immersion ageing in distilled water (corresponding batch is called Immersion). Ageing is conducted over a period of six weeks. The humidity in the chambers is controlled thanks to saturated salt solutions. The salt used and the exact relative humidity condition, controlled using testo 174H captors (Testo Inc., West Chester, USA), are presented in Table 1.

Table 1. Salt used for conditioning the chambers and the exact relative humidity condition induced by them.

	Temp. [°C]	**50% RH**	**75% RH**	**98% RH**
Mean value [%]	23.3 ± 2.2	55.7 ± 2.9	77.2 ± 1.9	99.7 ± 0.8
Salt used	/	$Mg(NO_3)_2$	NaCl	K_2SO_4

Five samples of each batch are regularly weighted to obtain the weight evolution. After six weeks, once their weight stabilises, the 50_RH / 75_RH / 98_RH / Immersion samples are dried at 40°C until stabilisation. This drying step allows avoiding the hysteresis consideration of flax fibre sorption [6]. Finally, all samples are stabilised again at 50% RH. This ageing protocol is summarized in Figure 1. The difference between the 50_RH_ref and the 50_RH batches remains in the drying and restabilisation step, which are not applied to the 50_RH_ref samples. All the ageing protocol is done at room temperature. In the following discussions, wet samples (or wet state) will refer to the samples in saturated state during ageing. The restabilised samples (or restabilised state) will refer to the samples that have undergone ageing, drying and restabilisation at 50% RH.

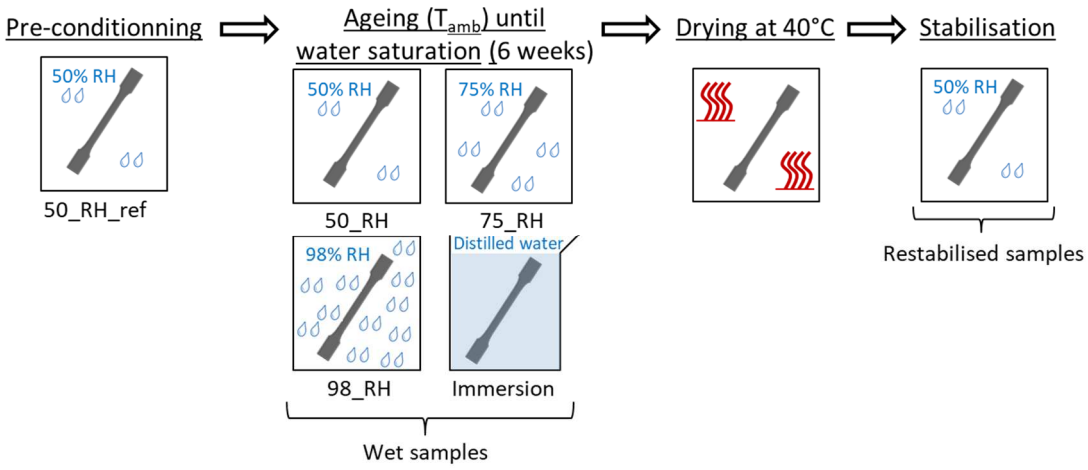

Figure 1. Schematic representation of the ageing protocol applied to a flax/PLA non-woven composite with a fibre volume fraction of 36%.

2.2.2 Water content

As described before, samples are regularly weighted using a Fisherbrand™ (Fisher Scientific SAS, Illkirch Cedex, France) scientific high precision scale having a precision of 10^{-4} g. The sampling depends on the stage of composite sorption, being narrow at the beginning of the sorption phenomenon. The moisture content at a given time (Mc(t)) is calculated from the weight evolution using equation (1).

$$M_c(t) = \frac{W(t) - W_{dry}}{W_{dry}} \quad \text{(Equ.1)}$$

Where *W(t)* is the sample weight at time *t* and W_{dry} is its dry weight. The dry weight of each sample is calculated equal to 97.4% of the initial mass of the samples as the initial moisture content was measured to be 2.6%. It avoids the drying step for samples before ageing, as it impacts the materials [22].

The sorption kinetics of the samples during ageing is discussed using Fick's law [11], equation (2), where D_{diff} is the diffusion coefficient, and *h* is the sample thickness. The initial moisture content and the moisture content at saturation are $M_{c,init}$ and M_∞, respectively. They are extracted from the experimental data for each ageing condition.

$$M_c(t) = (M_\infty - M_{c,init}).\left(1 - \frac{8}{\pi^2}\sum_{n=0}^{\infty}\frac{1}{(2n+1)^2}.exp^{\frac{-\pi^2.(2n+1)^2.D_{diff}.t}{h^2}}\right) + M_{c,init} \quad \text{(Equ.2)}$$

The diffusion coefficient (D_{diff}) is calculated for all experimental points in the linear part of the experimental curves ($M_c(t) < 0.5M_\infty$) using equation (3). The mean diffusion coefficient is used to implement Fick's law, equation (2).

$$D_{diff} = \pi.\frac{h^2}{16.t}.\left(\frac{M_c(t) - M_{c,init}}{M_\infty}\right) \quad \text{(Equ.3)}$$

2.2.3 Mechanical characterisation through tensile tests

A universal Instron (Instron, Norwood, Massachusetts, USA) tensile machine is used with a 10kN load cell. The tensile test is based on the ISO 527-4 standard, using a cross-head speed of 1 mm/min. The elongation of the samples is measured with an Instron extensometer having a gauge length of 25 mm. The stiffness is calculated between 0.02% and 0.1%. At least nine samples are tested, and the mean value is extracted. Standard deviations are used as errors. The tensile tests are only done on restabilised samples.

2.2.4 Density measurement

The density was obtained through a hydrostatic balance using ethanol as immersion liquid, leading to the density of the composites. Samples for density measurement are cut from the central part of the dog bone samples (2 x 8 x 45 mm) thank to a circular saw as it is the part loaded in the measurement of mechanical properties. This extraction is done on restabilised samples. Density results are given as mean values of at least five samples.

Thanks to the apparent density of the composite (ρ_c), the volume fraction of porosity (V_p) of each batch is estimated using equation (4). The weight fraction of fibres W_f are 40% here. The density of PLA (ρ_{PLA}) and flax (ρ_{flax}) are taken respectively as 1.24 and 1.5 gcm^{-3} [1]. This flax density value was measured at room temperature and 50RH. The flax fibres were extracted from unidirectional preforms made for composite applications.

$$V_p = 1 - \left(\frac{1 - W_f}{\rho_{PLA}} + \frac{W_f}{\rho_{flax}} \right) . \rho_c \qquad \text{(Equ.4)}$$

The assumption of an unchanged fibre density during ageing is taken. The porosity induced by manufacturing will be considered as matrix pores, and the porosity due to ageing will be referred to as defects, or specifically matrix micro-cracks or interface decohesion zones.

2.2.5 SEM

Samples are observed thanks to a JEOL (Jeol, Tokyo, Japan) SEM (JSM-IT500HRSEM) at an acceleration voltage of 3 kV. For transverse section observation, sample preparation consists of embedding them into an epoxy matrix, polishing and gold-coating thanks to a sputter coater (Edward Scancoat6). For flax/PLA interface observation, samples underwent a brittle fracture under nitrogen before being sputter coated. Any surface degradation was observed, skipping the embedding step as polishing is not desirable.

2.2.6 Biochemical analysis

Biochemical analysis is done on the immersion leachate to quantify the polysaccharides released by the composite. Before undergoing biochemical analysis, the leachate was centrifuged (3min at 800 rpm). Three samples of supernatants (500µL) were collected. First, 2-déoxy-D-ribose is added before samples are hydrolysed (2h at 120°C). Then, the uronic acid (UA) concentration was determined by an automated m-hydroxybiphenyl method [23]. Additionally, the neutral sugar concentration was analysed as their alditol acetate derivatives [24] by GC gas chromatography (PerkinElmer, Clarus 580, Shelton, CT, USA) equipped with a DB 225 capillary column (J&W Scientific, Folsorn, CA, USA) at 205°C, with H_2 as the carrier gas.

2.2.7 AFM

A Multimode 8 AFM instrument (Bruker, Billerica, Massachusetts, USA) was used in PF-QNM imaging mode. This mode is based on the recording of force-distance curves at a high rate (2 kHz) for a limited maximum load (200 nN here), and thus limited indentation depth (of the order of a nanometre here), while the tip scans the surface of the sample thus allowing to make topography maps. The indentation modulus is obtained from the unloading part of the force-distance curve using an appropriate contact model. We used a DMT model here, which corresponds to the Hertz contact model (small indentation depth compared to the tip apex

radius) modified to take into account the adhesion force (mainly due to water capillarity in our case) between the tip and the sample surface [25]. The indentation modulus obtained is similar to that obtained by nanoindentation measurements but with the required resolution to study mechanical gradients within and between cell wall layers [26]. RTESPA-525 (Bruker) silicon probe with a spherical tip apex was used here. Its spring constant (between 136 and 177 N/m) was calibrated using the Sader method (https://sadermethod.org/), and the tip radius adjusted between 20 and 80 nm on an aramid sample having a comparable indentation modulus to flax fibre cell walls. Image resolution of 384×384 pixels was achieved, and a peak force amplitude between 50 and 100 nm was set for indentation modulus measurements. This variety of amplitude depends on the roughness of the region investigated.

Only the reference, the 98_RH and the immersion batches were investigated in regards to the mechanical properties, the density results and the SEM observation. AFM samples of 2 mm^3 are extracted from the middle of the centre part of the dog bones. It avoids edge influence. They are embedded into agar resin (Agar Scientific, Stansted, UK) and cut thanks to an ultramicrotome (Leica Ultracut R). Four images, including of flax fibres and PLA, were used for each reference to obtain the mean indentation modulus of the reinforcement and the matrix. The samples were analysed in a perpendicular plane of the direction with the predominant orientation of fibres (machine direction of the preform). For flax fibres, which are highly anisotropic, elliptical fibre cross-sections were not selected to avoid the risk of fibre misorientation.

3 Results and discussion

3.1 Moisture content evolution

The moisture content at saturation of the composite stored at 50% RH is 2.6 ± 0.1 %. As expected for flax composite, the moisture sorption at room temperature follows Fick's law

[18,27] (pseudo-Fickian behaviour for immersion), as presented in Figure 1. The parameters used for Fick's law are extracted from the experimental curves and are given in Table 2.

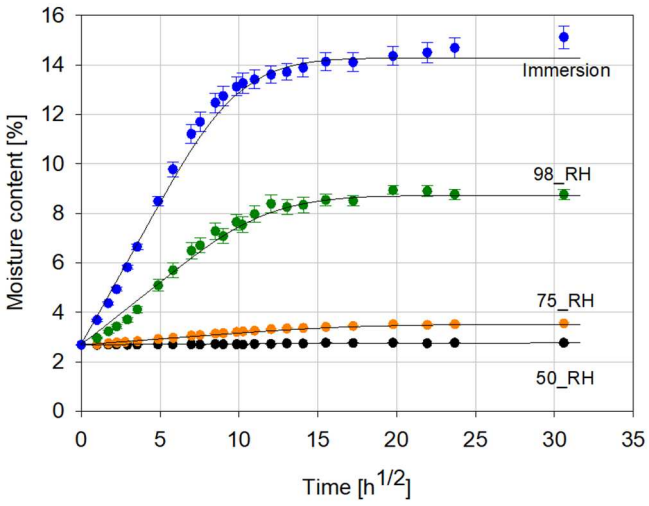

Figure 2. Moisture content evolution of a non-woven flax/PLA composite (Wf=40%) under several ageing conditions. The dark lines correspond to Fick's laws extrapolation. The experimental curves are used to obtain the diffusion coefficients and the moisture content at saturation.

Table 2. Parameters used to calculate Fick's law, depending on the ageing condition.

	50_RH	**75_RH**	**98_RH**	**Immersion**
$D_{diff}.10^{-6}$ [mm²/s]	0.56	0.72	1.53	2.15
M_∞ [%]	2.77	3.52	8.72	14.275

The moisture contents at saturation after each ageing step can be observed in Figure 2. No clear saturation is reached in the case of immersion. Before discussing the results, note that the stabilised moisture content of flax fibres is measured by Hill et al. [6] to be 18% at 95% RH.

The water uptake of virgin PLA under immersion at 25°C was measured by Deroiné et al. [28] to be 0.59 ± 0.03% . This low moisture sorption is explained by the high glass transition temperature of PLA (60°C) [29]. As our flax/PLA composite uptakes 15.12 ± 0.46% after 38 days (30 $h^{1/2}$) of moisture under immersion at room temperature, it can be concluded that flax fibres and/or composite microstructure (matrix pores/defects induced by ageing) are principally responsible for moisture uptake. As a consequence, PLA moisture sorption is not considered in any further detail in this work.

Besides a slightly higher moisture content at saturation, the moisture uptake behaviour of 50_RH and 75_RH are similar, as observed in Table 3. The moisture uptake appears to be more critical for the 98_RH and immersion samples. The sorption behaviour of flax fibres can explain this. It has been reported by Gouanvé et al. [8] that the mechanism of sorption of flax fibres evolves after a relative humidity close to 80%. Water molecules are absorbed on specific interaction sites or randomly adsorbed by flax, and thereafter, the water molecules cluster in the interstice and porosity of flax fibres, such as lumen or cell wall micropores [8]. Such micropores have been observed by Melelli et al. [30] on flax kink bands, where the flax structure is more heterogeneous and presents significant cavities compared to intact cell walls. This phenomenon is also observed for composites [5], where the matrix pores and the interfaces (matrix/fibres or fibres/fibres) are other places for potential water clustering.

Regarding the drying and restabilisation step, all batches return to a moisture content slightly higher than their initial moisture content of 2.6 ± 0.1 %, except the immersion one. Interestingly, the 98_RH samples lose more water during the drying step, meaning it has potentially a higher free/bonded water ratio than the 75_RH and 50_RH batches.

Table 3. Moisture content in non-woven flax/PLA composite (Wf=40%) at each ageing step for all the ageing conditions. Index a, b, c highlight statistical groups determine by comparative t-tests (p-value > 0.05 in a same group).

		50_RH	75_RH	98_RH	Immersion
Water content at saturation [-]	ageing	2.77 ± 0.01 %	3.55 ± 0.04 %	8.76 ± 0.21 %	15.12 ± 0.46 %
	drying	1.46 ± 0.04 %	1.59 ± 0.05 %	1.17 ± 0.11 %	0.24 ± 0.07 %
	restabilisation	2.72 ± 0.02 % [a]	2.88 ± 0.03 % [b]	2.86 ± 0.09 % [b]	1.94 ± 0.05 % [c]

The difference between mean water content at restabilisation is checked with t-tests. It appears that statistically, only 75_RH and 98_RH have an identical mean value. In the case of immersion, the moisture content after ageing and restabilisation is lower than the initial moisture content.

3.2 Leaching phenomenon

The difference of water uptake for immersed samples is mainly due to a decrease in the sample weight, distorting the moisture content value. Considering that the moisture content of the immersed samples after stabilisation should be similar to other ageing conditions (ca 2.7-2.9%), this weight loss equals ca 0.8-1.0%.

This decrease can be induced by a leaching phenomenon already reported in the literature [31]. It is confirmed by a change in the colour of the leachate during immersion ageing. Some polysaccharides of the flax are dissolved and released in the surrounding water. The total mass of samples immersed is 40 g in one litre of distilled water. Thus, considering leaching as the only origin of the mass evolution (taken equals to 0.9%), the weight loss should induce a sugar concentration of 360 µg/mL. However, thanks to biochemical analysis of the leachate, the total sugar concentration only equals 25.7 µg/mL. This concentration includes 18.9 µg/mL of neutral sugars and 6.8 µg/mL of uronic acids. The detailed biochemical analysis of the leachate is given

275 in Table 4.

276 **Table 4.** Biochemical analysis of the leachate obtained after flax/PLA non-woven composite
277 immersion ageing. Rha = Rhamnose, Fuc= Fucose, Ara= Arabinose, Xyl= Xylose, Man=Mannose,
278 Gal=Galactose, Glc=Glucose; U.A. = Uronic acids. N/A refers to undetected sugars.

	Rha	**Fuc**	**Ara**	**Xyl**	**Man**	**Gal**	**Glc**	**U.A.**
Concentration [µg/mL]	4.6 ± 1.6	N/A	N/A	N/A	N/A	5.2 ± 1.7	9.1 ± 4.4	6.8 ± 0.3

279

280 As dissolved polysaccharides alone cannot explain all the weight loss, PLA degradation due to
281 fibre swelling at the surface is assumed to have a role [32]. The surface degradation is
282 observed through SEM in Figure 3. Interestingly, the composite manufacturing process
283 exposes flax fibres on the surface (face and edge) of unaged composites, see Figure 3. These
284 fibres are a preferential path for water molecules, influencing the sorption kinetics observed in
285 Figure 2.

286 3.3 Surface degradation

287 Additionally, an increase in degradation is observed qualitatively from the reference to
288 immersion samples (see Figures 3.a, 3.b). Indeed, the surface roughness increases, highlighting
289 the contribution of flax fibres swelling due to surface degradation. Additionally, cracks are
290 reported close to the fibres, confirming PLA damaged by flax swelling.

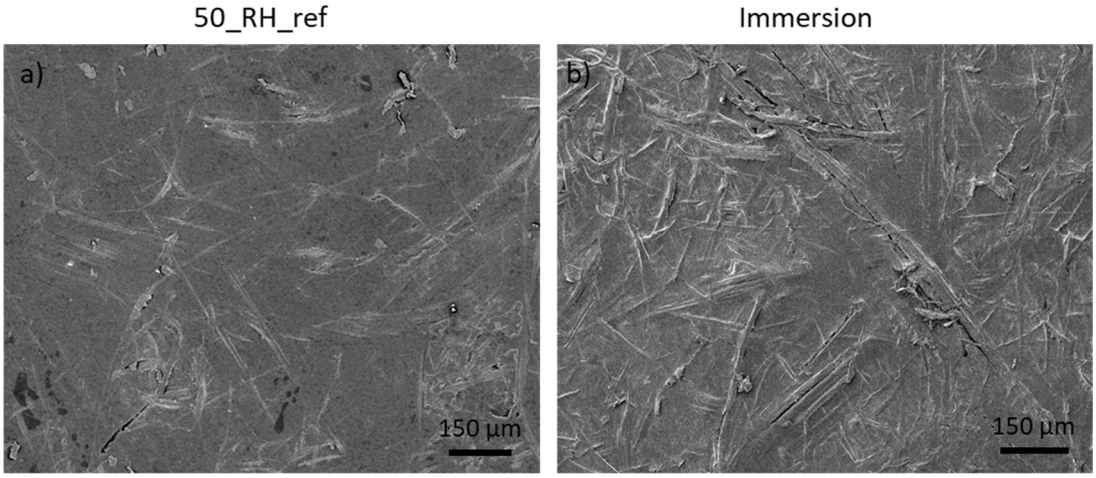

Figure 3. Perpendicular SEM observation of the surface degradation for 50_RH_ref (a) and immersion (b) samples, focussing on the role of flax fibre swelling.

The surface degradation is more evident through tilted observation of the surfaces, highlighting the presence of flax fibres exposed at the surface, responsible for the higher roughness of the immersed samples. At a lower scale, as seen in Figures 4.c, 4.d, the reference sample presents few exposed fibres at the composite face/edge, which are still surrounded by PLA (see Figure 4.c). This is due to the manufacturing process which does not include the presence of extra PLA layer on the edges. The number of exposed flax fibres in the immersion samples appear higher, and they are locally detached from the PLA as gaps are present (see Figure 4.d). They can even be uncoupled from PLA in some cases. It highlights the surface degradation and liberation of PLA micro-particles, explaining also the weight loss.

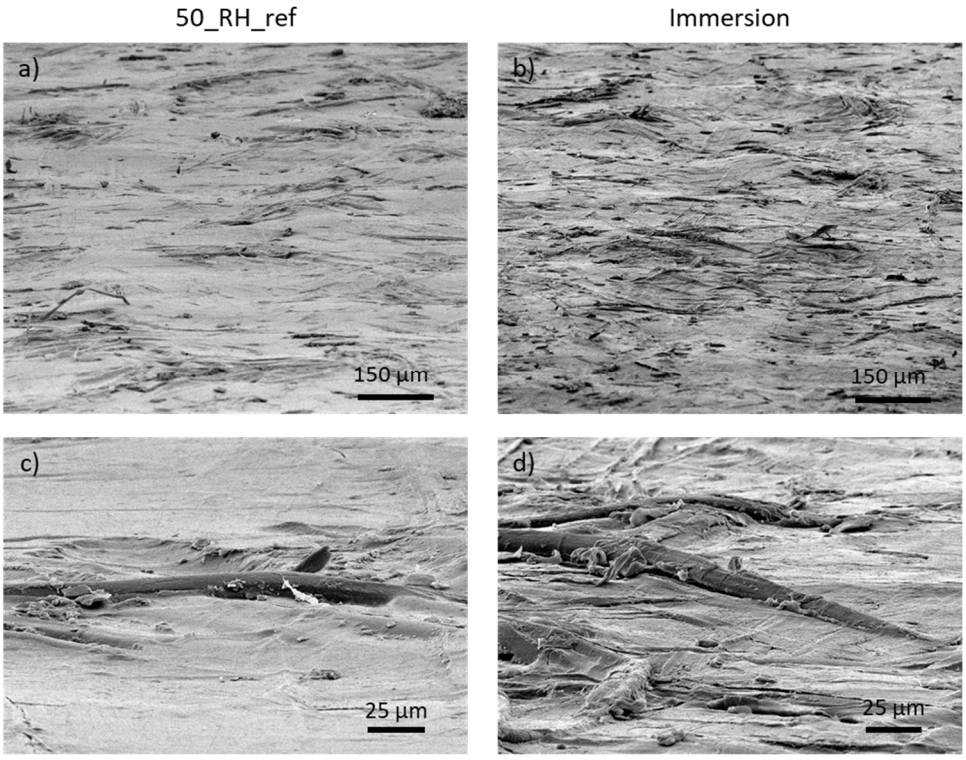

Figure 4. Tilt SEM observation of surface degradation for 50_RH_ref (a & c) and immersion (b & d) samples. a) & b) are global views of the surface aspect, c) & d) focus on the aspect of exposed flax fibres.

3.4 Tensile properties

By testing the mechanical properties of restabilised samples, their irreversible alteration induced by water sorption is assessed. The tensile behaviours are represented in Figure 4.a and the mechanical properties are summarised in Table 5. The 50_RH and 75_RH samples do not present significant differences with the 50_RH_ref batch, as they present similar tensile behaviour (Figure 4.a). That means the drying step (40°C until stabilisation) does not impact the reference composite, and ageing at 75% RH does not induce irreversible change in the flax/PLA composite. However, a decrease in stiffness and strength are observed for the 98_RH and immersion batches (Figure 4. b)), with a stiffness decrease of 20.3% for 98_RH and 33.4%

for immersion. It agrees with the moisture uptake of wet samples, which is much higher for 98_RH and immersion than for the three undamaged batches.

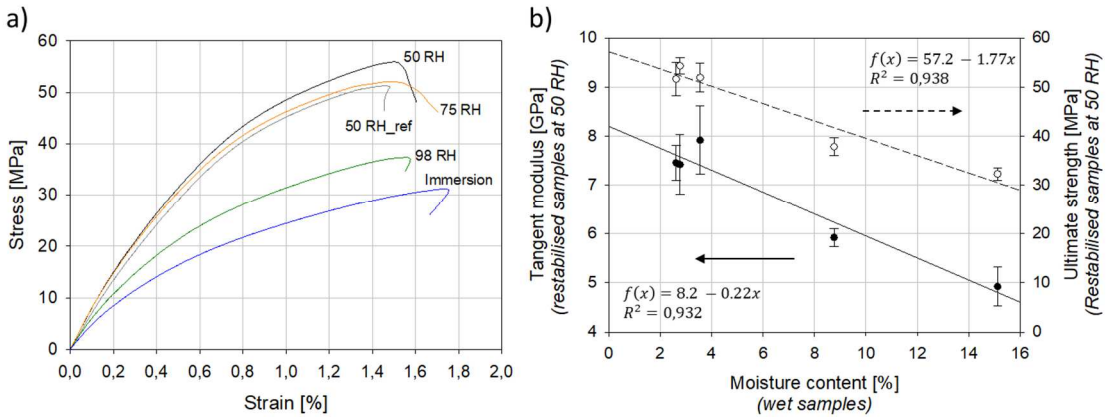

Figure 5. a) Tensile behaviour of flax/PLA composite (Wf=40%) after ageing under several conditions, drying and restabilisation at 50% RH (restabilised state), b) Influence of moisture content at saturation (wet state) on the tensile properties of the flax/PLA composite after ageing, drying and restabilisation at 50% RH (restabilised state).

Interestingly, the decrease in mechanical properties of restabilised samples appears to directly depend on the moisture content in the wet state (mainly due to the damage created by the water uptake), as reported in Figure 4.b. These trends approach a linear correlation, with a decrease factor of 1.77 MPa/% for strength and 0.22GPa/% for the modulus. This linearity might be due to the progressive increase of defects inside the composite induced by the moisture content. These linear decreases were also observed for an injected PLA/flax immersed in seawater [33], and an increase in defects in the composite was assumed.

Interestingly, the strain of the composite remains around 1.6 – 1.8% (Table 5) even for 98_RH

and immersed samples, which is in the same range as the failure strain of the flax fibre, 2.1 ± 0.5% [34]. Thus, composite behaviour is still fibre dominated even after ageing. The decrease appears similar to fibre volume reduction, indicated a loss of interface and therefore a loss of stress transfer ability from fibre.

It highlights the existence of a critical relative humidity between 75% RH and 98% RH (see Figure 5), where flax composites present irreversible damage. The moisture content of flax composites is described by a sigmoid [5,8] as the water starts to sorb at specific sites of interaction, then in non-specific sites before clustering micro-pores become present in flax fibres (lumen or kink-bands). A relative humidity close to 80% RH induces a drastic increase in water content in flax fibres and therefore inside the composite. This relative humidity is probably the limit to not reach to avoid irreversible damage in the composite, but its exact value may depend on the matrix mechanical behaviour. This critical relative humidity can be observed using more relative humidity ageing between 75% RH and 98% RH. Additionally, it will help to identify more precisely the nature of the trend. The dry states (lower than 2.6%) can result in different damage mechanisms, leading to another modification of mechanical properties not highlighted by the presented trend Figure 5.).

Interestingly, the water molecules change from the gas phase to the liquid phase when the saturation pressure of water is reached. It occurs at the physical limits of relative humidity of 99.9%. For the flax/PLA non-woven composite, the moisture content jumps from 9% to 15% by switching from 98% RH to immersion ageing. Therefore, the moisture content range of 9% to 15% is not reachable. However, the impact of immersion on tensile properties appears to align with vapour ageing impact, as observed in Figure 4.b. The shortcut of immersion as accelerated vapour ageing should be used carefully as the water molecules are not in the same state. Thus, ageing mechanisms could be different between vapour and immersion conditions.

359 The latter is expected to be harsher.

360

361 **Table 5.** Tensile properties of flax/PLA composite (Wf=40%) after ageing under several
362 conditions, drying and reconditioning at 50% RH (restabilised state). The pure PLA values are
363 extracted from a previous study [35] and measured on unaged INGEO™ PLA samples.

	50_RH_ref	50_RH	75_RH	98_RH	Immersion	Pure PLA (unaged)
Tangent modulus [GPa]	7.4 ± 0.3	7.4 ± 0.6	7.9 ± 0.7	5.9 ± 0.2	4.9 ± 0.4	3.4 ± 0.1
Ultimate strength [MPa]	51.6 ± 3.3	54.3 ± 1.6	51.9 ± 3.0	37.8 ± 1.8	32.3 ± 1.3	37.6 ± 0.8
Strain at failure [%]	1.5 ± 0.2	1.5 ± 0.1	1.4 ± 0.1	1.6 ± 0.1	1.8 ± 0.3	2.6 ± 0.4

364

365 The amount of water uptake is the origin of composite degradation. Two hypotheses have to
366 be verified. First, contact with water can decrease the mechanical properties of the flax fibres
367 and the matrix. Indeed, the mechanical properties of elementary flax fibres depend on the
368 surrounding relative humidity [23], with a decrease in strength of ca. 15% and an increase of
369 ca. 25% of strain switching from 46% to 85% RH. Second, the composite structure can
370 deteriorate through decohesion of the flax and matrix or by creating matrix micro-cracks
371 induced by flax swelling and shrinkage. The combination of both phenomena will induce
372 connected defects. For example, the decohesion at the interface creates a gap between the
373 flax and the matrix. These gaps could be linked together by the micro-cracks present in the
374 matrix. The reduction in composite density can be used to quantify the volume of these
375 structural defects.

376 3.5 Evolution of flax cell wall and matrix stiffness in the composite

377 As expressed previously, one hypothesis is that ageing impacts the properties of flax and/or

the matrix. Therefore, their mechanical properties are assessed through AFM measurement on the reference and the two impacted batches. Figure 5 presents the indentation modulus mapping used for one measurement, whereas Table 6 presents the averaged indentation modulus for flax and PLA matrix.

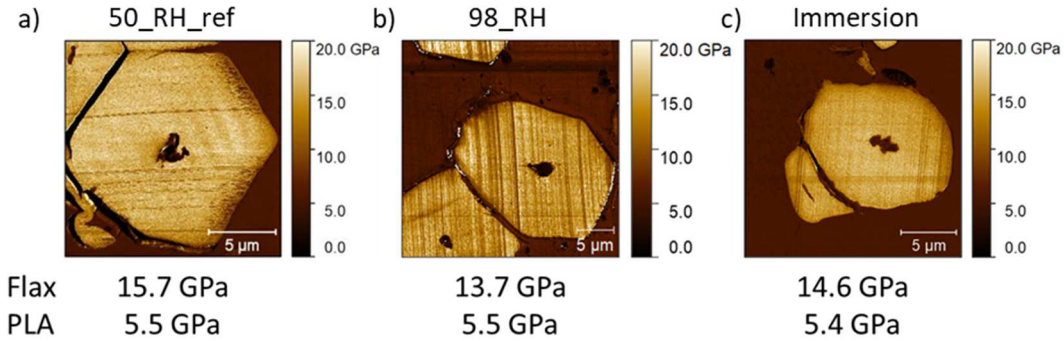

Figure 6. AFM indentation stiffness map for one fibre of flax/PLA composite after a) no ageing (50_RH_ref), b) moisture ageing at 98% RH, c) immersion ageing with distilled water.

The evolution of constituent mechanical properties is measured at microscale level. [b b] First, the mechanical properties of PLA do not evolve during ageing, with a constant indentation modulus value of ca. 5.5 GPa. Thus, there is no local recrystallisation of PLA. This is expected as PLA's stiffness is relatively insensitive to immersion ageing at 25°C [28]. Indeed, Deroiné et al. [28] reported, for virgin PLA aged six months in distilled water at 25°C, no decrease in mechanical properties at the macro-scale and only a small chemical evolution with a decrease of number-averaged molecular weight from 75,000 g/mol (unaged) to 66,300 g/mol.

Table 6. Impact of the ageing condition on the indentation stiffness of flax fibres cell walls and PLA in the composite. It is investigated at the micro-scale level through AFM-QNM measurements.

	50_RH_ref	98_RH	Immersion
Flax fibre indentation modulus [GPa]	15.3 ± 1.0	13.4 ± 1.8	13.9 ± 0.9
PLA indentation modulus [GPa]	5.5 ± 0.1	5.4 ± 0.3	5.4 ± 0.2

For the flax cell wall (the layer S2 of the secondary cell wall), a slight decrease appears between the reference and the impacted samples. The impacted samples (98_RH and immersion) are considered statistically identical, as a t-test gives a probability of similarity equals to 63%. However, due to the close value between the reference and the impacted samples, their standard deviation and the operator influence on the selection of the fibres, it can be concluded that flax cell walls present similar mechanical properties whatever the ageing condition used. Note that these values are slightly lower than the indentation modulus usually obtained in the literature using AFM, being between 17-22 GPa [36].

Interestingly, this stable indentation modulus does not agree with Le Duigou et al.'s [31] results from nanoindentation measurements on immersed unidirectional flax/PLA composite. Indeed, they observed a 40% decrease in nanoindentation modulus after four weeks, compared to a 10% decrease (without considering the standard deviation) after six weeks in this study. They explain the decrease of the mechanical properties by the solubilisation of uronic acids, playing a role in transferring loads in the second wall (S2) of the flax fibres [31]. They observed a ratio of 2.5 between the uronic acids released and the neutral sugars. Thanks to the biochemical analysis, this ratio is calculated to be 0.36 in our leachate, supporting the unchanged mechanical properties of the flax fibres in the immersed samples.

The difference between both experiments can be explained by the difference in flax preform and manufacturing process. Le Duigou et al. [31] used a vacuum film stacking method to manufacture flax/PLA unidirectional composite at a fibres weight fraction of 50%. This manufacturing method leads to lower compaction than the thermo-compression due to low pressure (≈ 0.95 bar) [37] and potentially modify flax fibres composition as it requires the severe manufacturing condition of 180°C for 1 hour. In addition, the unidirectional orientation of fibres leads to easier leaching than random orientation as fibre percolation in the composite is higher for unidirectional. Finally, they used a magnetic stirrer, which may increase the leaching phenomenon.

Thus, the evolution of flax cell walls and PLA's mechanical properties cannot explain the decrease in stiffness observed at the composite scale. Therefore, the second hypothesis relating to the evolution in composite microstructure (and density) should be investigated as it may be responsible for mechanical property evolution.

3.6 Composite density evolution

The structural modification of the composite through ageing is potentially due to the decohesion phenomenon or micro-cracks generation in the matrix, both being related to flax fibre swelling. These mechanisms are directly linked to the composite density, as they modify its structure by damaging the interfaces for the first one and creating matrix micro-cracks for the second. The density measurement is presented in Figure 6.a). The porosity estimated is presented in Figure 6.b), considering constant flax and matrix density. However, the assumption of a constant flax density is debatable as the moisture uptake and swelling phenomena can modify flax fibre structure (not observed here by AFM), where the leaching phenomenon (immersed samples only) modifies its biochemical composition.

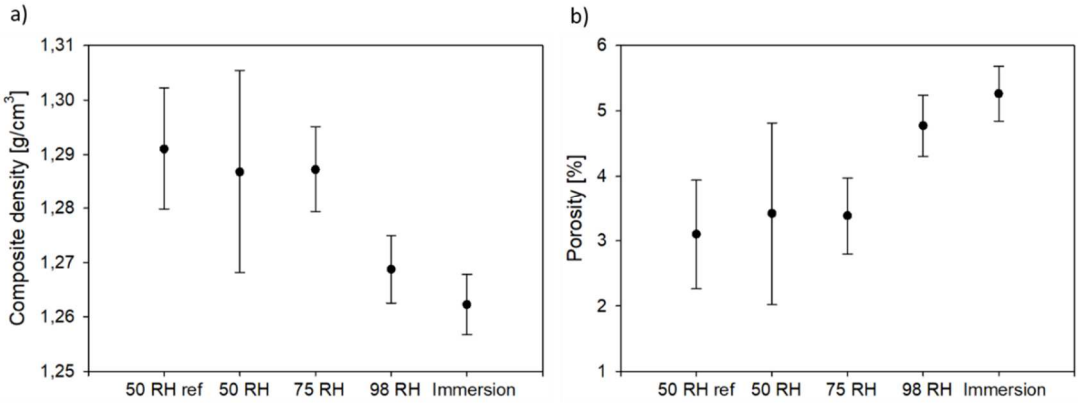

440

441 **Figure 7.** Evolution of the a) composite density and b) porosity of restabilised samples after
442 different ageing conditions. The porosity is calculated assuming ageing does not modify the
443 PLA nor flax density.

444

445 Nevertheless, the results fall in line with the mechanical properties evolution as the batches
446 with low density present the lowest mechanical properties. Indeed, the porosity appears to be
447 similar for the 50_RH_ref / 50_RH / 75_RH samples, increasing for 98_RH and Immersion
448 samples (see Figure 6.b). Thus, ageing induces a modification of the inner structure of the
449 composite. The origin of the structural modification needs further investigations to understand
450 its influence on mechanical properties.

451 3.7 Interface decohesion

452 First, interface cohesion is checked through SEM observation on cryo-fractured samples. The
453 obtained pictures are presented in Figure 7, presenting flax fibres in the normal direction of
454 the fracture. If a damage is observed, a physical decohesion can be identified. The embedded
455 length should not be considered here as these samples are observed before any tensile test.

456

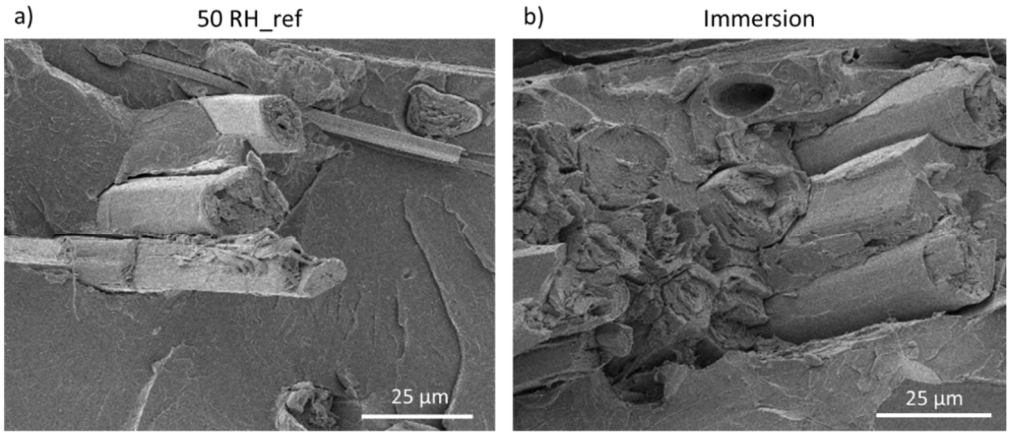

457

458 **Figure 8.** Interface observation by SEM of flax/PLA composite after a failure of the sample
459 under cryogenic condition, a) observation of the reference and b) observation of the most
460 damaged batches, being the immersion one. No decohesion is observed after an immersion
461 ageing as damage is present.

462

463 No significant decohesion at the flax/matrix or the flax/flax interfaces could be observed for
464 reference or aged flax/PLA composite. There are two explanations, the first being that the
465 interface is not damaged during ageing. One possibility is that fibres embedded within the PLA
466 in the core of the sample are not subjected to water uptake nor swelling. However, this is
467 unrealistic as the randomness of the preform induces interconnectivity of the flax fibres,
468 percolating the open edges in contact with the environment.

469 The second more realistic explanation is a damaged interface, but this could not be observed.
470 This damage can be due to chemical modification (leaching [31]) or hidden physical
471 decohesion. During the thermo-compression process, the flax fibres have a low water content
472 due to the high temperature. Thus, the flax fibres in the 50_RH_ref composite are already
473 constrained. In addition to the hygroscopic stress, some residual stresses due to the thermal

history of the polymer and flax fibres are present. In addition, flax fibres act as nucleating agents for the PLA, creating a transcrystalline layer around the fibres [38]; presence of water in the interface region, can also induce local hydrolysis of the PLA matrix.

During the ageing, the flax fibres swell enough to overcome the matrix's yield point locally and irreversibly deform the matrix. The drying step allows the flax fibres to retract as their water content decrease, damaging the interface and releasing the internal residual stresses. Through the restabilisation at 50% RH, the flax fibres are now free to swell, as the matrix did not constrain it, and fill the gap previously created, hiding the decohesion. This phenomenon, schematised in Figure 8, should not significantly modify the composite's density.

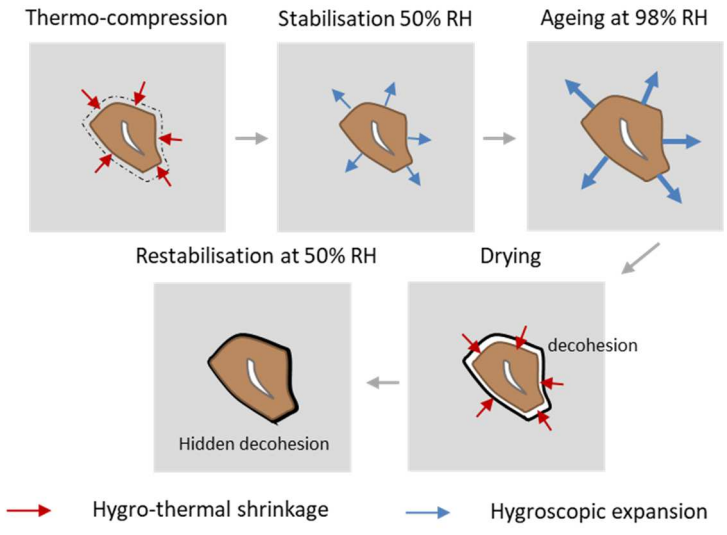

Figure 9. Schematic explanation of the formation of hidden decohesion due to the alternation of shrinkage and expansion of flax fibres inside the composite. Inspired from [9].

These potential damages at the interface can explain the decrease of the mechanical

properties of flax/PLA composite as the stress transfer between reinforcement and matrix. Consequently, the reinforcement of flax fibres is less efficient, inducing a decrease in the modulus and the ultimate strength of the composite without any increase in its ultimate strain.

3.8 Micro-cracks generation in the matrix

The swelling of the fibres during ageing has another consequence in the composite structure. As observed in Figure 10, the aged composite presents micro-cracks inside the matrix, initiated at the matrix/fibre interfaces. It suggests that the stresses applied locally by the swelled flax fibres to the matrix are higher than the ultimate strength of the matrix. Therefore, the presence of these micro-cracks decreases the mechanical properties of the composites. Indeed, they act as defects, lowering the ultimate strength of the composite but also reducing the apparent stiffness of the matrix.

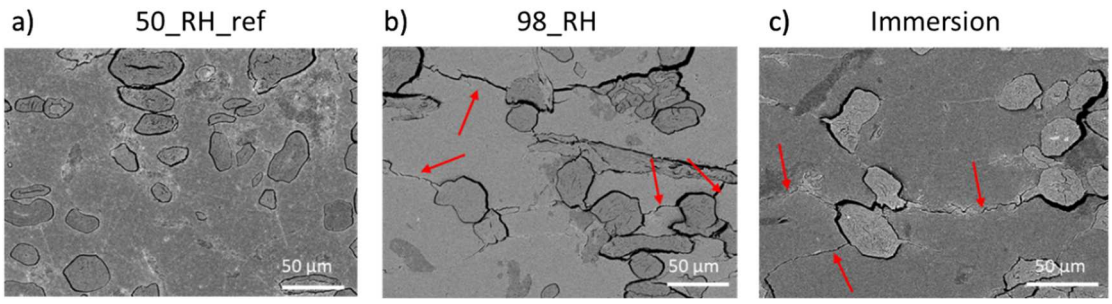

Figure 10. SEM observation of flax/PLA composite after a) no ageing, b) ageing at 98% RH, c) an immersion ageing. The observations are perpendicular to the direction of the sample. The red arrows focus on the presence of matrix micro-cracks. The samples are polished.

As a first approach, the stiffness of a random non-woven composite (E_{NW}) is estimated thanks

to $E_{NW} = \frac{3}{8}.E_{UD,longi} + \frac{5}{8}.E_{UD,transv}$, where $E_{UD,longi}$ and $E_{UD,transv}$ are the longitudinal and transversal stiffness of an equivalent unidirectional composite, respectively. The matrix stiffness is the predominant parameter of the unidirectional transversal stiffness [39]. Thus, the apparent matrix stiffness reduction due to micro-cracks directly decreases the transversal stiffness of an equivalent unidirectional composite, and so does the non-woven composite stiffness. In addition, a higher number of matrix micro-cracks might induce a lower apparent matrix stiffness. It has been observed in Figure 4.b) that the tensile stiffness of a dry sample depends on its moisture uptake in the wet state. As the number of micro-cracks should increase with higher moisture uptake (due to higher flax swelling), the generation of matrix micro-cracks is responsible for the decrease in the tensile stiffness of aged non-woven flax/PLA composites. Thus, these matrix micro-cracks decrease the composite strength but also its stiffness.

The fact that immersion ageing influences mechanical properties in line with vapour ageing indicates that the main damage mechanisms are mutual to immersion and vapour ageing. It can be the matrix micro-cracks or the hidden decohesion. The leaching phenomenon is discarded as it is specific to immersed samples.

Note that these micro-cracks were observed on epoxy embedded and polished samples (with water). The friction induced by polishing and water sorption at the surface could have been responsible for these cracks. However, the reference samples did not present micro-cracks. This gives confidence that these micro-cracks are created during ageing and not during the sample preparation. A CT-scan analysis could avoid this damaging effect and confirm the presence of the micro-cracks due to ageing. Such analysis could give additional information such as the number of matrix micro-cracks, their connectivity and their geometry. Furthermore, it can confirm the link between the number of matrix micro-cracks, the water

uptakes at the wet state and the tensile mechanical properties of the dry sample. However, that needs a high resolution as such micro-cracks have a thickness of no more than a few micrometres.

4 Conclusion

The evolution of the microstructure and the development of damage in a flax non-woven composite subjected to water ageing (at 50% RH / 75% RH / 98% RH / immersion) was investigated. The ageing conditions selected aimed to understand the first degradation step of a flax/PLA non-woven composite. The ageing process was monitored by following the composite's moisture content over six weeks and waiting for stabilisation in their weight before being dried and restabilised at 50% RH. Interestingly, ageing at 75% RH did not impact the mechanical properties nor the composite structure. On the other hand, samples aged at 98% RH and immersion for six weeks presented a significant uptake of water, decreasing the strength and stiffness of the composites significantly.

A deeper analysis was conducted to better understand the ageing mechanisms. AFM investigation in peak-force mode revealed that the flax fibre cell walls and the PLA appeared to keep their initial indentation moduli. Thus, any composite softening was due to an evolution of the composite’s structure, confirmed by increased porosity for the two impacted batches. The interface was observed thanks to the cryogenic failure of aged samples. No damage, including signs of decohesion of matrix and fibre, was observed. This may probably be due to the restabilisation step and the free swelling of fibres, closing (‘hiding’) debonding regions created by ageing. It appeared that the porosity increase was due to the creation of transverse micro-cracks induced by flax fibres swelling. That confirmed that the swelling of the fibres was responsible for the structural evolution of the composite, hidden decohesion or matrix micro-crack generation. These structural evolutions impacted the tensile properties of the flax/PLA

555 non-woven composite by decreasing its ultimate strength and stiffness.

556 On the one hand, investigating more relative humidity conditions in the range of 75RH and
557 98RH can help identify the presence of a critical relative humidity at which mechanical
558 properties and structure start to get significantly affected. Additionally, extending these
559 experimental investigations of flax/PLA non-woven composites with various fibres volume
560 fractions could lead to additional clues on the degradation mechanisms. Furthermore, using
561 cyclic tensile loading cycles could give information on the role of interfacial defects on the
562 composite mechanical behaviour. Finally, the effect of protecting the edges and the surface by
563 a thin PLA layer could be scientifically interesting as it is expected to reduce the sorption
564 kinetics, even if it is not realistic industrially speaking, unless for example using thermal
565 methods for machining (such as laser cutting).

566

567 **Acknowledgements**

568 The authors want to thank the INTERREG IV Cross Channel programme for funding this work
569 through the FLOWER project (Grant number 23).

570

571 **References**

572 [1] M. Le Gall, P. Davies, N. Martin, C. Baley, Recommended flax fibre density values for
573 composite property predictions, Industrial Crops and Products. 114 (2018) 52–58.
574 https://doi.org/10.1016/j.indcrop.2018.01.065.
575 [2] A. Lefeuvre, A. Bourmaud, C. Morvan, C. Baley, Tensile properties of elementary fibres of
576 flax and glass: Analysis of reproducibility and scattering, Materials Letters. 130 (2014)
577 289–291. https://doi.org/10.1016/j.matlet.2014.05.115.
578 [3] J. Holbery, D. Houston, Natural-fiber-reinforced polymer composites in automotive
579 applications, JOM. 58 (2006) 80–86. https://doi.org/10.1007/s11837-006-0234-2.
580 [4] F. Bensadoun, B. Vanderfeesten, I. Verpoest, A.W. Van Vuure, K. Van Acker,

581 Environmental impact assessment of end of life options for flax-MAPP composites,
582 Industrial Crops and Products. 94 (2016) 327–341.
583 https://doi.org/10.1016/j.indcrop.2016.09.006.
584 [5] V. Gager, A. Le Duigou, A. Bourmaud, F. Pierre, K. Behlouli, C. Baley, Understanding the
585 effect of moisture variation on the hygromechanical properties of porosity-controlled
586 nonwoven biocomposites, Polymer Testing. 78 (2019).
587 https://doi.org/10.1016/j.polymertesting.2019.105944.
588 [6] C.A.S. Hill, A. Norton, G. Newman, The water vapor sorption behavior of flax fibers—
589 Analysis using the parallel exponential kinetics model and determination of the
590 activation energies of sorption, Journal of Applied Polymer Science. 116 (2010) 2166–
591 2173. https://doi.org/10.1002/app.31819.
592 [7] S. Alix, E. Philippe, A. Bessadok, L. Lebrun, C. Morvan, S. Marais, Effect of chemical
593 treatments on water sorption and mechanical properties of flax fibres, Bioresource
594 Technology. 100 (2009) 4742–4749. https://doi.org/10.1016/j.biortech.2009.04.067.
595 [8] F. Gouanvé, S. Marais, A. Bessadok, D. Langevin, M. Métayer, Kinetics of water sorption
596 in flax and PET fibers, European Polymer Journal. 43 (2007) 586–598.
597 https://doi.org/10.1016/j.eurpolymj.2006.10.023.
598 [9] A. le Duigou, J. Merotte, A. Bourmaud, P. Davies, K. Belhouli, C. Baley, Hygroscopic
599 expansion: A key point to describe natural fibre/polymer matrix interface bond strength,
600 Composites Science and Technology. 151 (2017) 228–233.
601 https://doi.org/10.1016/j.compscitech.2017.08.028.
602 [10] A. Regazzi, S. Corn, P. Ienny, J.-C. Bénézet, A. Bergeret, Reversible and irreversible
603 changes in physical and mechanical properties of biocomposites during hydrothermal
604 aging, Industrial Crops and Products. 84 (2016) 358–365.
605 https://doi.org/10.1016/j.indcrop.2016.01.052.
606 [11] W.V. Srubar, C.W. Frank, S.L. Billington, Modeling the kinetics of water transport and
607 hydroexpansion in a lignocellulose-reinforced bacterial copolyester, Polymer. 53 (2012)
608 2152–2161. https://doi.org/10.1016/j.polymer.2012.03.036.
609 [12] Z. El Hachem, A. Célino, G. Challita, M.-J. Moya, S. Fréour, Hygroscopic multi-scale
610 behavior of polypropylene matrix reinforced with flax fibers, Industrial Crops and
611 Products. 140 (2019) 111634. https://doi.org/10.1016/j.indcrop.2019.111634.
612 [13] T. Joffre, E.L.G. Wernersson, A. Miettinen, C.L. Luengo Hendriks, E.K. Gamstedt, Swelling
613 of cellulose fibres in composite materials: Constraint effects of the surrounding matrix,
614 Composites Science and Technology. 74 (2013) 52–59.
615 https://doi.org/10.1016/j.compscitech.2012.10.006.
616 [14] M. Assarar, D. Scida, A. El Mahi, C. Poilâne, R. Ayad, Influence of water ageing on
617 mechanical properties and damage events of two reinforced composite materials: Flax–
618 fibres and glass–fibres, Materials & Design. 32 (2011) 788–795.
619 https://doi.org/10.1016/j.matdes.2010.07.024.
620 [15] G. Koolen, J. Soete, A.W. van Vuure, Interface modification and the influence on damage
621 development of flax fibre – Epoxy composites when subjected to hygroscopic cycling,
622 Materials Today: Proceedings. 31 (2020) S273–S279.
623 https://doi.org/10.1016/j.matpr.2020.01.183.

[16] T. Cadu, L. Van Schoors, O. Sicot, S. Moscardelli, L. Divet, S. Fontaine, Cyclic hygrothermal ageing of flax fibers' bundles and unidirectional flax/epoxy composite. Are bio-based reinforced composites so sensitive?, Industrial Crops and Products. 141 (2019) 111730. https://doi.org/10.1016/j.indcrop.2019.111730.
[17] L. Van Schoors, T. Cadu, S. Moscardelli, L. Divet, S. Fontaine, O. Sicot, Why cyclic hygrothermal ageing modifies the transverse mechanical properties of a unidirectional epoxy-flax fibres composite?, Industrial Crops and Products. 164 (2021) 113341. https://doi.org/10.1016/j.indcrop.2021.113341.
[18] A. Le Duigou, A. Bourmaud, P. Davies, C. Baley, Long term immersion in natural seawater of Flax/PLA biocomposite, Ocean Engineering. 90 (2014) 140–148. https://doi.org/10.1016/j.oceaneng.2014.07.021.
[19] A. Chilali, M. Assarar, W. Zouari, H. Kebir, R. Ayad, Effect of geometric dimensions and fibre orientation on 3D moisture diffusion in flax fibre reinforced thermoplastic and thermosetting composites, Composites Part A: Applied Science and Manufacturing. 95 (2017) 75–86. https://doi.org/10.1016/j.compositesa.2016.12.020.
[20] N. Martin, P. Davies, C. Baley, Evaluation of the potential of three non-woven flax fiber reinforcements: Spunlaced, needlepunched and paper process mats, Industrial Crops and Products. 83 (2016) 194–205. https://doi.org/10.1016/j.indcrop.2015.10.008.
[21] D. Pantaloni, D. Shah, C. Baley, A. Bourmaud, Monitoring of mechanical performances of flax non-woven biocomposites during a home compost degradation, Polymer Degradation and Stability. 177 (2020) 109166. https://doi.org/10.1016/j.polymdegradstab.2020.109166.
[22] C. Baley, A. Le Duigou, A. Bourmaud, P. Davies, Influence of drying on the mechanical behaviour of flax fibres and their unidirectional composites, Composites Part A: Applied Science and Manufacturing. 43 (2012) 1226–1233. https://doi.org/10.1016/j.compositesa.2012.03.005.
[23] A. Thuault, S. Eve, D. Blond, J. Bréard, M. Gomina, Effects of the hygrothermal environment on the mechanical properties of flax fibres, Journal of Composite Materials. 48 (2014) 1699–1707. https://doi.org/10.1177/0021998313490217.
[24] A.B. Blakeney, P.J. Harris, R.J. Henry, B.A. Stone, A simple and rapid preparation of alditol acetates for monosaccharide analysis, Carbohydrate Research. 113 (1983) 291–299. https://doi.org/10.1016/0008-6215(83)88244-5.
[25] K.L. Johnson, J.A. Greenwood, An Adhesion Map for the Contact of Elastic Spheres, Journal of Colloid and Interface Science. 192 (1997) 326–333. https://doi.org/10.1006/jcis.1997.4984.
[26] A. Melelli, O. Arnould, J. Beaugrand, A. Bourmaud, The Middle Lamella of Plant Fibers Used as Composite Reinforcement: Investigation by Atomic Force Microscopy, Molecules. 25 (2020) 632. https://doi.org/10.3390/molecules25030632.
[27] W. Wang, M. Sain, P.A. Cooper, Study of moisture absorption in natural fiber plastic composites, Composites Science and Technology. 66 (2006) 379–386. https://doi.org/10.1016/j.compscitech.2005.07.027.
[28] M. Deroiné, A. Le Duigou, Y.-M. Corre, P.-Y. Le Gac, P. Davies, G. César, S. Bruzaud, Accelerated ageing of polylactide in aqueous environments: Comparative study between

667 distilled water and seawater, Polymer Degradation and Stability. 108 (2014) 319–329.
668 https://doi.org/10.1016/j.polymdegradstab.2014.01.020.
669 [29] G. Francois, B. Stéphane, D. Guillaume, F. Pascale, C. Emmanuelle, G. Jeff, G. Régis, G.
670 Matthieu, H. Arnaud, L. Fabienne, others, Pollution des océans par les plastiques et les
671 microplastiques Pollution of oceans by plastics and microplastics, Techniques de
672 l'Ingenieur. (2020) BIO9300. https://archimer.ifremer.fr/doc/00663/77471/.
673 [30] A. Melelli, S. Durand, O. Arnould, E. Richely, S. Guessasma, F. Jamme, J. Beaugrand, A.
674 Bourmaud, Extensive investigation of the ultrastructure of kink-bands in flax fibres,
675 Industrial Crops and Products. 164 (2021) 113368.
676 https://doi.org/10.1016/j.indcrop.2021.113368.
677 [31] A. Le Duigou, A. Bourmaud, C. Baley, In-situ evaluation of flax fibre degradation during
678 water ageing, Industrial Crops and Products. 70 (2015) 204–210.
679 https://doi.org/10.1016/j.indcrop.2015.03.049.
680 [32] T. Bayerl, M. Geith, A.A. Somashekar, D. Bhattacharyya, Influence of fibre architecture on
681 the biodegradability of FLAX/PLA composites, International Biodeterioration &
682 Biodegradation. 96 (2014) 18–25. https://doi.org/10.1016/j.ibiod.2014.08.005.
683 [33] A. Le Duigou, P. Davies, C. Baley, Seawater ageing of flax/poly(lactic acid) biocomposites,
684 Polymer Degradation and Stability. 94 (2009) 1151–1162.
685 https://doi.org/10.1016/j.polymdegradstab.2009.03.025.
686 [34] C. Baley, A. Bourmaud, Average tensile properties of French elementary flax fibers,
687 Materials Letters. 122 (2014) 159–161. https://doi.org/10.1016/j.matlet.2014.02.030.
688 [35] D. Pantaloni, L. Ollier, D.U. Shah, C. Baley, E. Rondet, A. Bourmaud, Can we predict the
689 microstructure of a non-woven flax/PLA composite through assessment of anisotropy in
690 tensile properties?, Composites Science and Technology. 218 (2022) 109173.
691 https://doi.org/10.1016/j.compscitech.2021.109173.
692 [36] O. Arnould, D. Siniscalco, A. Bourmaud, A. Le Duigou, C. Baley, Better insight into the
693 nano-mechanical properties of flax fibre cell walls, Industrial Crops and Products. 97
694 (2017) 224–228. https://doi.org/10.1016/j.indcrop.2016.12.020.
695 [37] V. Popineau, A. Célino, M. Le Gall, L. Martineau, C. Baley, A. Le Duigou, Vacuum-Bag-Only
696 (VBO) Molding of Flax Fiber-reinforced Thermoplastic Composites for Naval Shipyards,
697 Appl Compos Mater. (2021). https://doi.org/10.1007/s10443-021-09890-2.
698 [38] S. Garkhail, B. Wieland, J. George, N. Soykeabkaew, T. Peijs, Transcrystallisation in PP/flax
699 composites and its effect on interfacial and mechanical properties, J Mater Sci. 44 (2009)
700 510–519. https://doi.org/10.1007/s10853-008-3089-9.
701 [39] I.M. Daniel, O. Ishai, Engineering mechanics of composite materials, 2nd ed, Oxford
702 University Press, New York, 2006.
703

704 **Figures captions**

705 **Figure 1.** Schematic representation of the ageing protocol applied to a flax/PLA non-woven

composite with a fibre volume fraction of 36%.

Figure 2. Moisture content evolution of a non-woven flax/PLA composite (Wf=40%) under several ageing conditions. The dark lines correspond to Fick's laws extrapolation. The experimental curves are used to obtain the diffusion coefficients and the moisture content at saturation.

Figure 3. Perpendicular SEM observation of the surface degradation for 50_RH_ref (a) and immersion (b) samples, focussing on the role of flax fibre swelling.

Figure 4. Tilt SEM observation of surface degradation for 50_RH_ref (a&c) and immersion (b&d) samples. a) & b) are global views of the surface aspect, c) & d) focus on the aspect of exposed flax fibres.

Figure 5. a) Tensile behaviour of flax/PLA composite (Wf=40%) after ageing under several conditions, drying and restabilisation at 50% RH (restabilised state), b) Influence of moisture content at saturation (wet state) on the tensile properties of the flax/PLA composite after ageing, drying and restabilisation at 50% RH (restabilised state).

Figure 6. AFM indentation stiffness map for one fibre of flax/PLA composite after a) no ageing (50_RH_ref), b) moisture ageing at 98% RH, c) immersion ageing with distilled water.

Figure 7. Evolution of the a) composite density and b) porosity of restabilised samples after different ageing conditions. The porosity is calculated assuming ageing does not modify the PLA nor flax density.

Figure 8. Interface observation by SEM of flax/PLA composite after a failure of the sample under cryogenic condition, a) observation of the reference and b) observation of the most damaged batches, being the immersion one. No decohesion is observed after an immersion

728 ageing as damage is present.

729 **Figure 9.** Schematic explanation of the formation of hidden decohesion due to the alternation
730 of shrinkage and expansion of flax fibres inside the composite. Inspired from [9].

731 **Figure 10.** SEM observation of flax/PLA composite after a) no ageing, b) ageing at 98% RH, c)
732 an immersion ageing. The observations are perpendicular to the direction of the sample. The
733 red arrows focus on the presence of matrix micro-cracks. The samples are polished.

734

735 **Tables Captions**

736 **Table 1.** Salt used for conditioning the chambers and the exact relative humidity condition
737 induced by them.

738 **Table 2.** Parameters used to calculate Fick's law, depending on the ageing condition.

739 **Table 3.** Moisture content in non-woven flax/PLA composite (Wf=40%) at each ageing step for
740 all the ageing conditions.

741 **Table 4.** Biochemical analysis of the leachate obtained after flax/PLA non-woven composite
742 immersion ageing. Rha = Rhamnose, Fuc= Fucose, Ara= Arabinose, Xyl= Xylose, Man=Mannose,
743 Gal=Galactose, Glc=Glucose; U.A. = Uronic acids. N/A refers to undetected sugars.

744 **Table 5.** Tensile properties of flax/PLA composite (Wf=40%) after ageing under several
745 conditions, drying and reconditioning at 50% RH (restabilised state). The pure PLA values are
746 extracted from a previous study [35] and measured on unaged INGEO^{TM} PLA samples.

747 **Table 6.** Impact of the ageing condition on the indentation stiffness of flax fibres cell walls and
748 PLA in the composite. It is investigated at the micro-scale level through AFM-QNM

749 measurements.